Gapless broadband terahertz emission from a germanium photoconductive emitter

Singh, A.; Pashkin, A.; Winnerl, S.; Helm, M.; Schneider, H.;

Originally published:

May 2018

ACS Photonics 5(2018), 2718-2723

DOI: https://doi.org/10.1021/acsphotonics.8b00460

Gapless broadband terahertz emission from a germanium photoconductive emitter

A. Singh,[1] A. Pashkin,[1] S. Winnerl,[1] M. Helm,[1,2] H. Schneider[1]

[1]Helmholtz-Zentrum Dresden-Rossendorf, 01328 Dresden, Germany
[2]Cfaed and Institute of Applied Physics, TU Dresden, 01062 Dresden, Germany

ABSTRACT:

Photoconductive terahertz (THz) emitters have been fulfilling many demands required for table-top THz time-domain spectroscopy up to 3-4 THz. In contrast to the widely used photoconductive materials such as GaAs and InGaAs, Ge is a non-polar semiconductor characterized by a gapless transmission in the THz region due to absence of one-phonon absorption. We present here the realization of a Ge-based photoconductive THz emitter with a smooth broadband spectrum extending up to 13 THz and compare its performance with a GaAs-based analogue. We show that the spectral bandwidth of the Ge emitter is limited mainly by the laser pulse width (65 fs) and, thus, can be potentially extended to even much higher THz frequencies.

Generating THz pulses using biased photoconductive (PC) switches is one of the most studied and commonly utilized techniques due to the compact size of THz emitters and their operation flexibility. Major applications of pulsed THz radiation include the study of physical phenomena in materials, nondestructive testing, and chemical identification using time-domain spectroscopic techniques.[1-4] The multi-octave spectral bandwidth of THz pulses makes them useful for a broad range of spectroscopic applications. Most common and efficient emitters are fabricated on GaAs which require near-infrared pulse pumping around 800 nm wavelength. This makes them compatible with Ti:sapphire lasers operating at 800 nm wavelength. To bring down the pump laser cost, below band gap excitation in GaAs and low-bandgap semiconductor InGaAs compatible with fiber lasers have been used.[5-6] Current PC emitters are reasonably efficient for time domain spectroscopy in the 0.1-3 THz spectral band, but for higher frequencies the performance drops drastically.[7-9] The drop in THz signal at higher frequencies is mainly due to THz absorption and screening by optical phonons in GaAs and InGaAs which are polar semiconductors. The polar character of the bonding in these crystals makes their optical phonon infrared active enabling them to absorb THz radiation at the transverse optical (TO) phonon resonance frequency and results in a strong reflectivity within the Reststrahlen band between the TO and longitudinal optical (LO) phonon frequencies. Therefore, the emission spectrum of GaAs-based PC emitters is typically limited to ~ 7 THz.[8] Optical rectification techniques using thin crystals have shown some advantage over PC emitters for frequencies above 3 THz. However, all nonlinear crystals used for optical rectification like GaP, ZnTe etc. are also polar and, therefore, THz absorption by optical phonons affects their spectrum too and their gapless spectrum is limited up to 7 THz.[10,11] There have been continuous efforts to increase the THz bandwidth by exploring new emission techniques, too.[12-17]

The first successful approach for the generation of a gapless THz spectra utilized four-wave mixing process in air plasma induced by mJ femtosecond pulses.[12] Further extension of this technique for a broadband field-resolved detection has enabled a gapless coverage of frequencies up to 10-20 THz for linear and nonlinear spectroscopic measurements.[13] The disadvantage of the air plasma technology is the necessity to use amplified Ti:Sa laser systems with pulse energies above 100 µJ and correspondingly with low repetition rates. A major breakthrough to overcome the frequency limitation

problem using conventional femtosecond oscillators with nJ pulse energies came in recent years by the new concept of converting ultrafast photoinjected spin current into THz charge current emitting THz radiation.[14, 15] The extremely small thickness of such spintronic emitters (just few nanometers) makes any absorption or screening effects negligible and enables the generation of gapless broadband THz spectra. However, PC emitters offer a number of advantages such as tailoring of THz fields using appropriate electrode designs as well as a fast electrical modulation of the emitted signal for sensitive lock-in detection that avoids the necessity to modulate the incoming optical beam using mechanical choppers or acousto/electro-optical modulators.[18]

Under usual operating condition a photoconducting substrate is pumped on one side and THz radiation propagates through the substrate and leaves it from the other side. Such simple transmission scheme offers convenient alignment and high collection efficiency of the emitted THz radiation. Therefore, a PC emitter in this geometry should not only be able to radiate THz efficiently but also transmit it without high losses. In case of GaAs emitters, strong TO phonon absorption around 8 THz limits the gapless spectrum bandwidth to frequencies below 8 THz. There have been attempts to avoid this problem by operating the emitter in a reflection mode, i.e., when THz radiated out from the front surface is collected. But it does not solve the problem completely, as even in reflection mode the TO phonon absorption and an efficient screening at the LO phonon frequency produce anomalies in the THz spectrum.[19-21] The THz emission by the LO phonon in polar semiconductors becomes especially pronounced in case of very high bias fields inherent to p-i-n diode structures resulting in a sharp peak in the emitted broadband THz spectrum.[22] A true gapless broadband PC emitter covering frequencies up to more than 8 THz has still not been realized.

A PC emitter based on a non-polar semiconductor such as Si or Ge can potentially produce a gapless broadband THz spectrum spanning beyond the limit of 7-8 THz. Although Si-on-Sapphire PC switches were historically among the first THz emitters,[23] most of the modern devices are based on III-V semiconductors (GaAs and InGaAs) due to their higher carrier mobility as compared to Si. In contrast to Si, Ge exhibits much higher carrier mobility that is almost comparable to GaAs (see table 1) and is capable of supporting high photocurrents. Moreover, due to its small bandgap Ge can be excited using fiber lasers similar to InGaAs emitters. However, due to the indirect bandgap of Ge, its recombination time is of the order of μs. Probably, this has prevented Ge from getting attention as a PC material for THz emission since for an efficient operation the carrier lifetime should be much shorter than the time period between two pulses used to pump the emitter. There were few reports on THz emission from Ge using different techniques, but these emitters were not efficient and the reported spectral bandwidth was below 3 THz.[24, 25] Although for pulsed THz emission picosecond recombination and trapping times are not mandatory, they can be attractive to improve the performance of a THz emitter.[26] It was demonstrated that ultrashort carrier lifetimes in Ge thin films can be achieved by ion implantation.[25] Moreover, recently thermally evaporated Ge films featuring sub-ps trapping times have been reported.[27]

Here we present broadband THz emission from Ge PC emitter with a gapless spectrum. We demonstrate that the efficiency of the Ge emitter is comparable to an identical semi-insulating GaAs-based PC device and its bandwidth surpasses GaAs by more than factor of 2. Considering the progress in germanium-on-silicon for integrated silicon photonics, Ge is a material with better compatibility to the existing Si electronics as compared to any other THz material for integrating like GaAs, InGaAs, InAs, InSb, GaP, ZnTe, GaSe, etc. Strain engineered direct and indirect bandgap in Ge gives it further advantage to diversify its compatibility with different fiber lasers.[28-30]

RESULTS AND DISCUSSION

THz PC emitters are fabricated on nominally undoped Ge and semi-insulating GaAs substrates with the thickness of 625 µm and 500 µm, respectively. Fig. 1 shows transmission spectra of these substrates. The spectrum of the GaAs substrate is dominated by the strong absorption band between 7 and 10 THz where the transmission drops below the noise level (~ 0.2%) of the spectrometer. Obviously, it corresponds to the Reststrahlen band of GaAs defined by the TO and LO phonons. In addition there are two weaker absorption bands centered around 5 and 13 THz due to two-phonon absorption processes.[31] These features clearly limits the bandwidth of GaAs-based THz emitters. The Ge substrate shows high and almost flat transmittance, apart from a dip around 10 THz due to two-phonon absorption in Ge which is present even in non-polar semiconductors.[32] However, this high-order absorption processes in Ge are much weaker compared to the TO phonon absorption in GaAs and they should become almost negligible by thinning down the substrate to 100-200 µm.

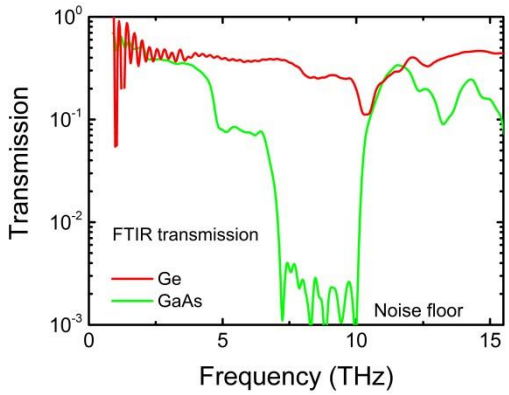

Fig. 1. Infrared transmission spectra of 650 µm GaAs and 500 µm Ge substrates.

To test the THz emission characteristics, the emitters are pumped with 800 nm NIR pulses of width ~ 65 fs, energy of 12 nJ at the repetition rate of 250 kHz. The pump pulse photo-generates electron-hole pairs in Ge (and GaAs) and these new charge carriers give rise to a current surge in biased emitter electrodes. This current surge causes the THz radiation. The next pump pulse comes after 4 µs, which gives enough time for carrier recombination and hence reduction in the photocurrent current before the arrival of next pump pulse. THz pulses emitted from GaAs and Ge recorded using 300 µm thick GaP are shown in Fig 2.(a) together with their Fourier transforms (Fig. 2b). The emitted THz field should be directly proportional to the sum of electron and hole mobility ($\mu_e + \mu_h$). Carrier mobility and bandgap of GaAs and Ge are listed in table 1. The carrier mobility sum ($\mu_e + \mu_h$) in Ge amounts to ~65 % of the value in GaAs, which is comparable to the peak electric field ratio of ~ 74% for the emitted THz pulses shown in Fig. 2(a).

The THz cut-off frequency for GaAs emitter is ~ 6.5 THz, which matches well with previous results on GaAs based PC emitters when tested with 400 µm thick GaP.[8] Low transmission in the 5-10 THz band in FTIR data in Fig.1 explains the cut-off frequency for GaAs emitters. The Fourier transform of THz radiation from Ge is broader than that of GaAs and extends up to 7.5 THz. The THz cut off beyond 7.5 THz in the Ge substrate is not expected from FTIR transmission data, so it could be due to the detector response. The electro-optic detection response of the GaP crystal at THz frequencies is calculated as described in ref.[33] and is plotted in Fig. 2. (c). The response function shows a drastic reduction beyond ~ 7.5 THz where the detector response is smaller by factor of 20 as compared to the

response at low frequency (< 1 THz). This means that the measured spectral bandwidth of the Ge emitter is limited by the detector response and the actual bandwidth of the THz radiation could be broader than observed by this detector as discussed below.

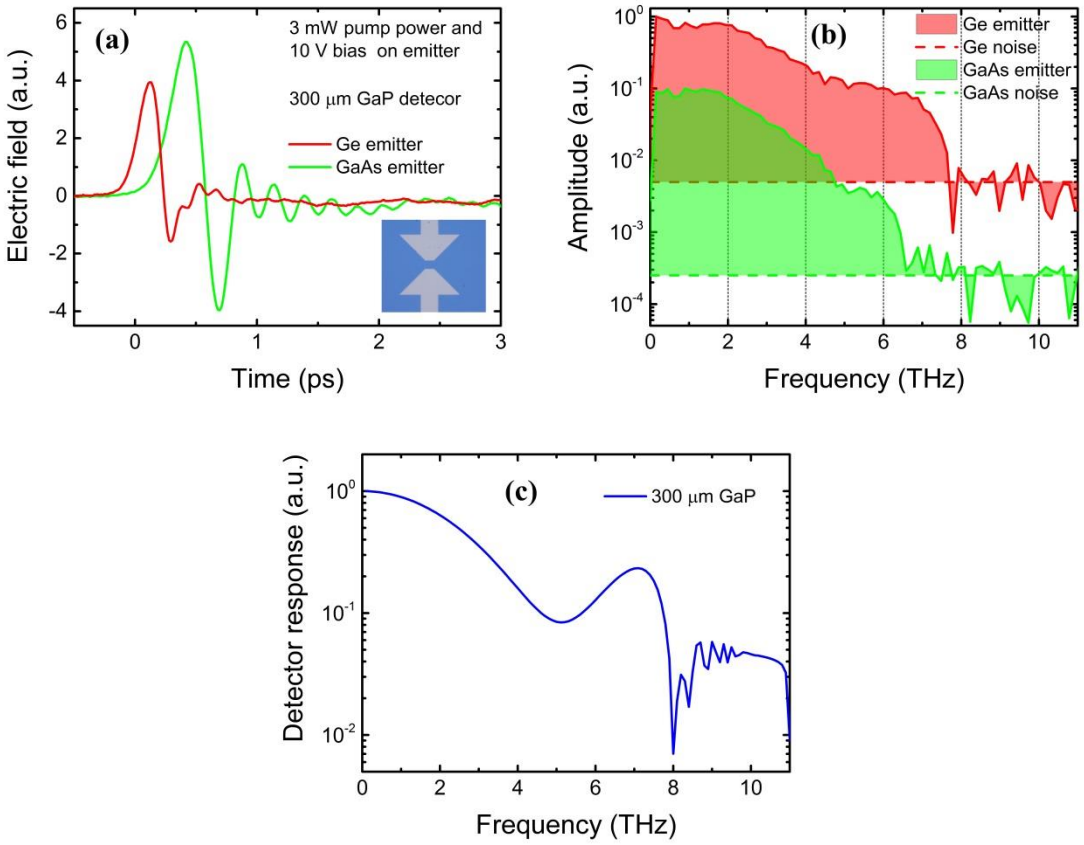

Fig. 2. (a) THz electric field recorded by 300 μm thick GaP. Optical microscope image of the bowtie electrode structure is shown in the inset. Gap between the two electrodes is 10 μm. (b) Normalized Fourier spectra of the THz pulses shown in (a). Fourier spectra are vertically shifted for visual clarity. (c) Calculated detector response function of 300 μm thick GaP.

Emitter performances are compared at different applied bias and different pump powers. Results are shown in Fig. 3 (a-c). Both emitters show saturation with the pump power at around 2 mW. The THz field dependence as a function of the applied bias field on the emitter is linear in GaAs which is expected. In Ge emitters this dependence appears slightly super-linear. This could be due to faster removal of photo-generated charge carriers from the substrate into the electrodes before arrival of the next pump pulse at the higher applied d.c. field, and hence reducing the off-state current (dark current) before the pump pulse. This should give a larger than expected current difference before and after the pump pulse excitation as the applied d.c. field increases. Potentially the effect of the fast removal of photo-generated carriers into the electrodes could be useful for high repetition rate pulse laser pumping. Another possibility is that it may be just due to non-Ohmic contact of the metal electrodes with the Ge substrate. It would be interesting to further investigate this behavior of the Ge emitters.

In electro-optic detection the group velocity of the sampling pulse should match the phase velocity of the THz pulse, otherwise the sampling pulse averages the THz electric field with respect to the different propagation delay between the two pulses. This limits the detector response at higher frequencies. To overcome this problem thin crystals are used, such that probe pulse and THz pulse do not get enough optical length for significant relative displacement while passing through the electro-

optic detector crystal. To test the emitter performance at higher THz frequencies, THz pulses are recorded using a 40 µm thick ZnTe<110> crystal. The detector response for this crystal is also calculated by the same method as in ref.[33] and it is plotted in Fig. 4 (b) with a solid black line.

Table.1. Carrier mobility and bandgap comparison of GaAs and Ge.[34,35]

	Bandgap (eV)	Electron mobility μ_e ($cm^2V^{-1}s^{-1}$)	Hole mobility μ_h ($cm^2V^{-1}s^{-1}$)	$\mu_e + \mu_h$ ($cm^2V^{-1}s^{-1}$)
GaAs	1.424	≤8500	≤400	≤8900
Ge	0.661 (0.8 at $E_{\Gamma 1}$ direct bandgap)	≤3900	≤1900	≤5800

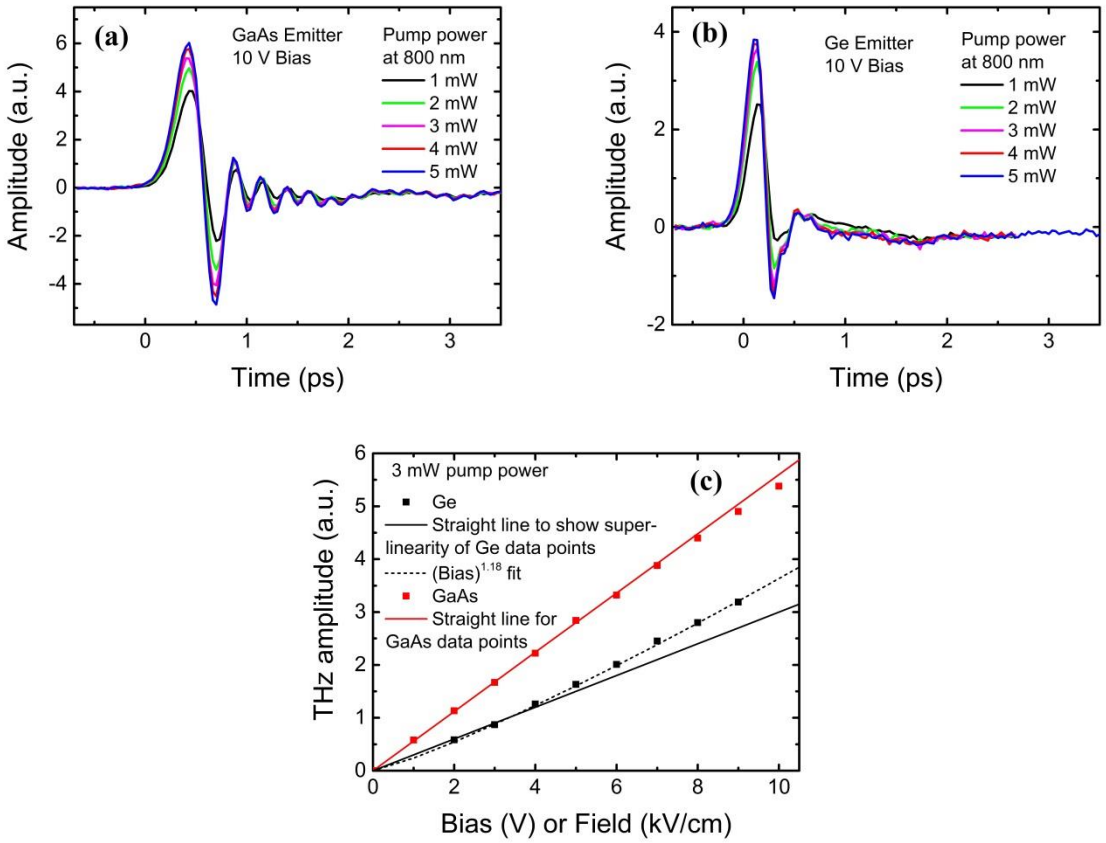

Fig. 3. (a) THz pulse recorded at different pump power for GaAs emitters. (b) THz pulse recorded at different pump power for Ge emitters. Both emitters show saturation in THz field enhancement with pump power at around 2 mW. (c) Variation of peak electric field with applied electric field on emitters. The field from the GaAs emitter shows a linear dependence on applied electric field as expected, whereas the THz field from the Ge emitter shows a superlinear trend with applied field ($(bias)^{1.18}$).

The sharp dip around 5 THz is due to a phonon resonance occurring in ZnTe. THz pulses recorded with 40 µm ZnTe are shown in Fig. 4(a). At the same applied bias of 10 V and pump power of 3 mW, the peak-to-peak electric field of the Ge pulse is very close to that of GaAs. Total carrier mobility ($\mu_e + \mu_h$) is higher in GaAs than Ge, but as discussed above, the GaAs substrate absorbs most of the THz intensity in the 7-10 THz band, making the THz electric field profile broader with reduced peak electric field. 40 µm ZnTe is thin enough to detect ultrafast electric field variations corresponding to

frequencies in the 7-10 THz band, which was not possible that efficiently when using 300 μm thick GaP. Therefore the THz signal from the Ge emitter is improved as compared to the THz signal from the GaAs emitter.

Fourier transforms of the THz pulses recorded with 40 μm ZnTe are shown in Fig. 4(c). Curves are shifted vertically for visual clarity. There is a strong dip at ~ 5 THz in both spectra which is due to the dip in detector response function as shown in Fig. 4(b). As expected from the FTIR data there is almost no signal beyond 5 THz for the GaAs emitter, whereas the spectrum of the Ge emitter extends up to 13 THz. The data in Fig. 4(c) also include the detector response variation with frequency. To obtain the actual spectrum of the emitted THz pulses, the detector response needs to be eliminated by dividing the measured spectrum amplitude by the detector response function. The detector response function is theoretically calculated and it has a very sharp dip around 5 THz. But this dip will not appear that sharp in the experimentally measured spectrum due to limited frequency resolution imposed by the extension of the measured trace in the time domain. To account for the frequency resolution, the calculated detector response function is convoluted with the frequency resolution function of our THz setup defined by the temporal interval used for electro-optic sampling (dash line curve in Fig 4 (b)). Measured spectra are divided by the convoluted detector response of Fig 4 (b) and the corrected FFT spectra are plotted in Fig. 4(d). For the Ge emitter the THz signal extends up to 13 THz, so the corresponding THz spectrum has been corrected up to 15 THz. The noise floor beyond 15 THz is divided by the value of the response function at 15 THz (~ 0.27) to preserve the continuity of the FFT curve. For the GaAs emitter, a clear signal is visible only up to 5 THz and the signal disappears completely beyond 7 THz. The FTIR measurement also shows almost no transmission across the GaAs substrate in the 7-10 THz band, so it is reasonable enough to consider the FFT amplitude at 7 THz to be the noise level for the GaAs emitter. Therefore the FFT spectrum is corrected only up to 7.5 THz, and the noise floor beyond 7.5 THz is divided by the detector response at 7.5 THz (~ 0.19).

In Fig. 4(d) we see a gapless exponentially decaying spectrum reaching up to 13 THz from the Ge emitter, which is far better than that of GaAs emitter at frequencies above 5 THz. The residual non-uniformity in the spectrum around 5 THz is due to incomplete compensation of the sharp dip in the detector response. The detector response is smooth around 10 THz; therefore the dip in the spectrum at 10 THz is considered real and attributed to the two-phonon absorption dip of Ge as also observed in the FTIR spectrum (see Fig. 1). The observation of this absorption feature in the THz spectrum demonstrates that its intensity is well above the noise level at these frequencies. Finally, we compare the measured THz spectrum with a THz spectrum for an idealized infinitely broadband emitter and a hypothetic detector which is limited only by the duration of our laser pulses (65 fs) used for photoexcitation and electro-optic detection. This idealized spectrum is shown in Fig. 4(d) by the black dashed line. Since the transformation due to the focusing optics is not taken into account, the spectral intensity remains finite down to zero frequency. The comparison with the experimental spectra shows good agreement and demonstrates that the high-frequency cut-off limit of the Ge emitter is mainly defined by the pulse duration of the laser amplifier system used in our experiment. Thus, the utilization of much shorter laser pulses from Ti:sapphire oscillators can potentially extend the bandwidth of Ge PC emitters above 20-30 THz or even higher.

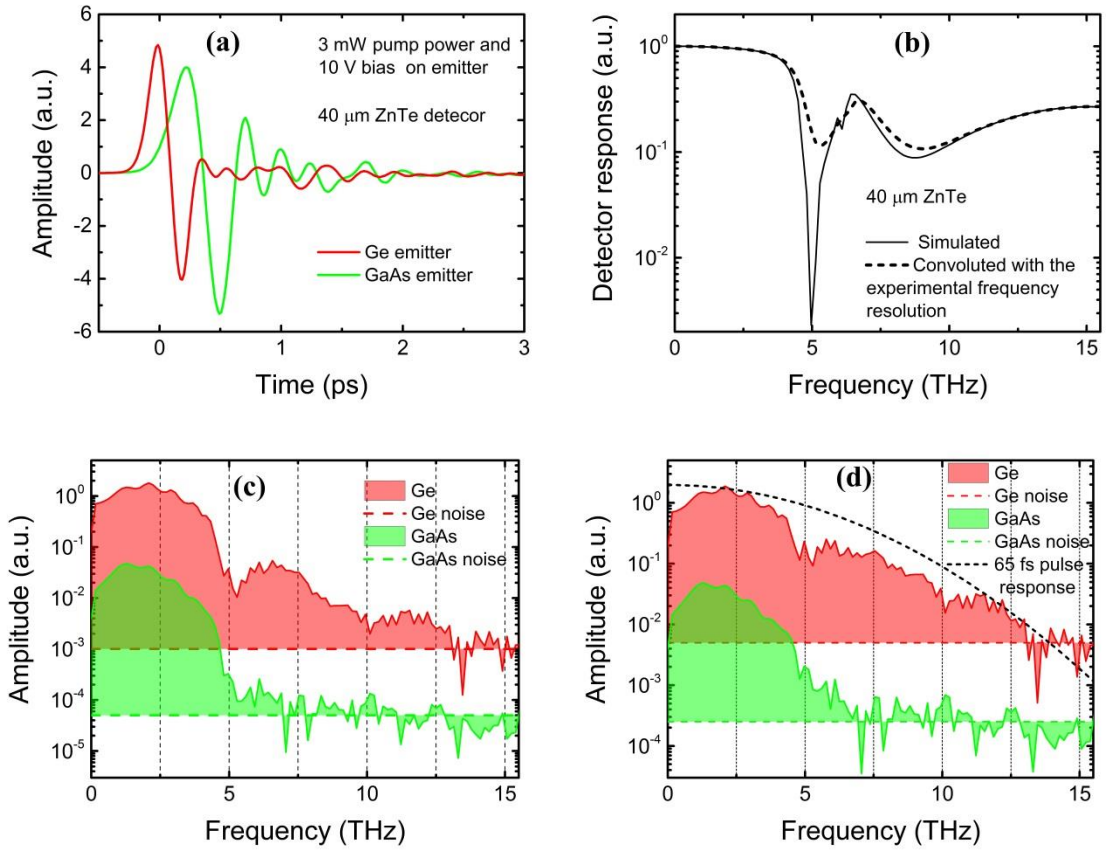

Fig. 4 (a) Electric field of the THz pulse from Ge and GaAs emitters recorded using 40 μm thick ZnTe. The THz pulse from Ge is sharper than that of GaAs. (b) Calculated electro-optic detection response function for 40 μm thick ZnTe. The calculated curve without taking into account any frequency resolution effect is shown as a black solid line. The calculated detector response function is convoluted with the experimental frequency resolution and the convoluted curve is plotted with dashed line. (c) FFTs of the THz pulses shown in (a). (d) FFT spectrum after correcting for the detector response function convoluted with the experimental frequency resolution. The dashed line represents an idealized spectrum limited only by the 65 fs duration of the laser pulses.

CONCLUSION

In conclusion, we successfully demonstrated the operation of a Ge photoconductive emitter as a THz emitter which is capable of radiating a true gapless spectrum up to 13 THz when pumped with 65 fs laser pulses. The emitted spectrum approaches a nearly ideal THz emitter and it is limited only by the laser pulse duration. In particular, provides broadband THz emission in the frequency range between 5 and 10 THz which is hardly accessible by common methods. Our results demonstrate the superior potential of Ge as a THz photoconductive material, with additional Si CMOS compatibility and longer cutoff wavelengths for the pump laser, and opens a new door for further investigations.

EXPERIMANTAL METHODS

Emitter Fabrication: An electron beam lithography technique is used to fabricate the electrode structures on Ge and GaAs. We fabricate standard bowtie like electrode structures to apply the bias in the semiconductor. The electrode gap is 10 μm. Both emitters have identical electrode structure. 45 nm thick Au on top of 5 nm Ti is deposited by electron beam evaporation on the substrate to fabricate the electrodes.

FTIR Measurements: Transmission spectra of GaAs and Ge substrates are measured using a Fourier-transform infrared (FTIR) spectrometer (Bruker Vertex80v).

THz TDS measurement: A standard THz time domain spectroscopy setup using off-axis parabolic mirrors is used to record the THz pulses. A Ti-Sapphire amplifier laser with wavelength centered around 800 nm, pulse width ~ 65 fs and 250 kHz repetition rate is used to pump the emitters, and part of the same laser pulse is used for electro optic sampling of the emitted THz pulse field. Emitters are tested in transmission mode. The frequency resolution of the FFT spectrum depends on the THz pulse span used to take the Fourier transform, which is 6.66 ps for plots in Fig.2 and 6.30 ps for plots in Fig. 4.

ACKNOWLEDGMENT: Support by the Nanofabrication Facilities Rossendorf at IBC is gratefully acknowledged.

References:

1. Basov, D. M.; Averitt, R. D.; van der Marel, D.; Dressel, M.; Haule, K. Electrodynamics of correlated electron materials. *Rev. Mod. Phys.* **2011,** 83, 471−541.
2. Ulbricht, R; Hendry, E.; Shan, J.; Heinz, T. F.; Bonn, M. Carrier dynamics in semiconductors studied with time-resolved terahertz spectroscopy. *Rev. Mod. Phys.* **2011,** 83, 543−586.
3. Tonouchi, M. Cutting-edge terahertz technology, *Nat. Photonics* **2007,** 1(2), 97–105.
4. Siegel, P. Terahertz technology in biology and medicine. *IEEE Trans. Microw. Theory Tech.* **2004,** 52(10), 2438–2447.
5. Fesharaki, F.; Jooshesh, A.; Bahrami-Yekta, V.; Mahtab, M.; Tiedje, T.; Darcie, T. E.; Gordon, R. Plasmonic Antireflection Coating for Photoconductive Terahertz Generation. *ACS Photonics* **2017,** 4, 1350−1354.
6. Jooshesh, A.; Bahrami-Yekta, V.; Zhang, J.; Tiedje, T.; Darcie, T. E.; Gordon, R. Plasmon-Enhanced below Bandgap Photoconductive Terahertz Generation and Detection. *Nano Lett.* **2015,** 15 (12), 8306–8310.
7. Globisch, B.; Dietz, R. J. B.; Kohlhaas, R. B.; Göbel, T.; Schell, M.; Alcer, D.; Semtsiv, M.; Masselink, W. T. Iron doped InGaAs: Competitive THz emitters and detectors fabricated from the same photoconductor. *J. Appl. Phys.* **2017,** 121, 053102.
8. Klatt, G.; Gebs, R.; Janke, C.; Dekorsy, T.; Bartels, A. Rapid-scanning terahertz precision spectrometer with more than 6 THz spectral coverage. *Opt. Express* **2009,** 17, 25, 22847-22854.
9. Dreyhaupt, A.; Winnerl, S.; Dekorsy, T.; Helm, M. High-intensity terahertz radiation from a microstructured large-area photoconductor. *Appl. Phys. Lett.* **2005,** 86(12), 121114.
10. Huber, R.; Brodschelm, A.; Tauser, F.; Leitenstorfer, A. Generation and field-resolved detection of femtosecond electromagnetic pulses tunable up to 41 THz. *Appl. Phys. Lett.* **2000,** 76, 3191-3193.
11. Aoki, K.; Savolainen, J.; Havenith, M. Broadband terahertz pulse generation by optical rectification in GaP crystals. *Appl. Phys. Lett.* **2017,** 110, 201103.
12. Cook, D. J.; Hochstrasser, R. M. Intense terahertz pulses by four-wave rectification in air. *Opt. Lett.* **2000**, 25, 1210-1212.
13. Clough, B.; Dai, J.; Zhang, X.-C. Laser air photonics: beyond the terahertz gap. *Materials Today* **2012**, 15, 50-58.
14. Seifert, T.; Jaiswal, S.; Martens, U.; Hannegan, J.; Braun, L.; Maldonado, P.; Freimuth, F.; Kronenberg, A.; Henrizi, J.; Radu, I.; Beaurepaire, E.; Mokrousov, Y.; Oppeneer, P. M.;

Jourdan, M.; Jakob, G.; Turchinovich, D.; Hayden, L. M.; Wolf, M.; Münzenberg, M.; Kläui, M.; Kampfrath, T. Efficient metallic spintronic emitters of ultrabroadband terahertz radiation. *Nat. Photonics* **2016,** 10, 483-488.

15. Kampfrath, T.; Battiato, M.; Maldonado, P.; Eilers, G.; Nötzold, J.; Mährlein, S.; Zbarsky, V.; Freimuth, F.; Mokrousov, Y.; Blügel, S.; Wolf, M.; Radu, I.; Oppeneer P. M.; Münzenberg, M. Terahertz spin current pulses controlled by magnetic heterostructures. *Nature Nanotech.* **2013,** 8, 256–260.
16. Luo, L.; Chatzakis, I.; Wang, J.; Niesler, F.B.P.; Wegener, M.; Koschny, T.; Soukoulis.; C. M. Broadband terahertz generation from metamaterials. *Nat. Commun.***2014,** 5:3055.
17. Zhang, Y.; Zhang, X.; Li, S.; Gu, J.; Li, Y.; Tian, Z.; Ouyang, C.; He, M.; Han, J.; Zhang, W. Broadband THz-TDS System Based on DSTMS Emitter and LTG InGaAs/InAlAs Photoconductive Antenna Detector. *Sci. Rep.* **2016,** 6, 26949.
18. Winnerl, S.; Zimmermann, B.; Peter, F.; Schneider, H.; Helm, M. Terahertz Bessel-Gauss beams of radial and azimuthal polarization from microstructured photoconductive antennas. *Opt. Express* **2009,** 17, 1571-1576.
19. Shen, Y. C.; Upadhya, P. C.; Linfield, E. H.; Beere, H. E.; Davies, A. G.; Ultrabroadband terahertz radiation from low-temperature-grown GaAs photoconductive emitters. *Appl. Phys. Lett.* **2003,** 83, 3117-3119.
20. Shen, Y. C.; Upadhya, P. C.; E. H.; Beere, Linfield, E. H.; Davies, A. G.; Gregory, I. S.; Baker, C.; Tribe, W. R.; Evans, M. J.; Generation and detection of ultrabroadband terahertz radiation using photoconductive emitters and receivers. *Appl. Phys. Lett.* **2004,** 85(2), 164–166.
21. Hale, P. J.; Madeo, J.; Chin, C.; Dillon, S.S.; Mangeney, J.; Tignon, J.; Dani, K. M. 20 THz broadband generation using semi-insulating GaAs interdigitated photoconductive antennas. *Opt. Express* **2014,** 22, 26358–26364.
22. Leitenstorfer, A.; Hunsche, S.; Shah, J.; Nuss, M. C.; Knox, W. H. Femtosecond Charge Transport in Polar Semiconductors. *Phys. Rev. Lett.* 1999, 82, 25, 5140-5143.
23. Auston, D. H.; Cheung, K. P.; Smith, P. R. Picosecond photoconducting Hertzian dipoles. *Appl. Phys. Lett.* **1984,** 45, 284-286.
24. Kang, C.; Leem, J. W.; Maeng, I.; Kim, T. H.; Lee, J.S.; Yu, J. S.; Kee, C. S. Strong emission of terahertz radiation from nanostructured Ge surfaces. *Appl. Phys. Lett.* **2015,** 106, 261106.
25. Sekine, N.; Hirakawa, K.; Sogawa, F.; Arakawa, Y.; Usami, N.; Shiraki, Y.; Katoda, T. Ultrashort lifetime photocarriers in Ge thin films. *Appl. Phys. Lett.* **1996,** 68, 3419-3421.
26. Singh, A.; Pal, S.; Surdi, H.; Prabhu, S. S.; Nanal, V.; Pillay, R. G. Highly efficient and electrically robust carbon irradiated semi-insulating GaAs based photoconductive terahertz emitters. *Appl. Phys. Lett.* **2014,** 104, 063501.
27. Lim, W. X.; Manjappa, M.; Srivastava, Y. K.; Cong, L.; Kumar, A.; MacDonald, K. F.; Singh, R. Ultrafast All-Optical Switching of Germanium-Based Flexible Metaphotonic Devices. *Adv. Mater.* **2018**, 30, 1705331
28. Michel, J.; Liu, J.; Kimerling, L. C. High-performance Ge-on-Si photodetectors. *Nat. Photonics* **2010,** 4, 527-534.
29. Fang, Y. Y.; Tolle, J.; Roucka, R.; Chizmeshya, A. V. G.; Kouvetakis, J. Perfectly tetragonal, tensile-strained Ge on $Ge_{1-y}Sn_y$ buffered Si(100). *Appl. Phys. Lett.* **2007,** 90, 061915.
30. Fang, Y. Y.; Tolle, J.; Tice, J.; Chizmeshya, A. V. G.; Kouvetakis, J.; D'Costa, V. R.; Menéndez, J. Epitaxy-driven synthesis of elemental Ge/Si strain-engineered materials and device structures via designer molecular chemistry. *Chem. Mater.* **2007,** 19, 5910–5925.
31. Jamshidi, H.; Parker, T. J., Patel, C.; Sherman, W. F. Observation and assignment of phonon combination bands in the far infrared dielectric response of GaAs. *J. Mol. Struct.* **1984,** 113, 277-280

32. Deinzer, G.; Strauch, D. Two-phonon infrared absorption spectra of germanium and silicon calculated from first principles. *Phys. Rev. B* **2004,** 69, 045205.
33. Leitenstorfer, A.; Hunsche, S.; Shah, J.; Nuss, M. C.; Knox, W. H. Detectors and sources for ultrabroadband electro-optic sampling: Experiment and theory. *Appl. Phys. Lett.* **1999,** 74, 1516-1518.
34. Blakemore, J. S. Semiconducting and other major properties of gallium arsenide. *J. Appl. Phys.* **1982,** 53, R123-R181.
35. Jacoboni, C.; Nava, F.; Canali, C.; Ottaviani, G. Electron drift velocity and diffusivity in germanium. *Phys. Rev. B* **1981,** 24, 2, 1014-1026.